Cytokinin response factors regulate auxin-mediated organogenesis

Mária Šimášková,[1,2] José Antonio O'Brien,[1,2] Mamoona Khan,[3] Giel Van Noorden,[1,2] Krisztina Ötvös,[3] Anne Vieten,[4] Inge De Clercq,[1,2] Johanna Maria Adriana Van Haperen,[5] Candela Cuesta,[3] Klára Hoyerová,[6] Steffen Vanneste,[1,2] Peter Marhavý,[3] Krzysztof Wabnik,[3] Frank Van Breusegem,[1,2], Moritz Nowak,[1,2], Angus Murphy,[7] Jiří Friml,[1,3] Dolf Weijers,[5] Tom Beeckman,[1,2] and Eva Benková[1,3,*]

[1]Department of Plant Systems Biology, VIB, Technologiepark 927, B-9052 Gent, Belgium

[2]Department of Plant Biotechnology and Bioinformatics, Ghent University, Technologiepark 927, B-9052 Gent, Belgium

[3]Institute of Science and Technology Austria (IST Autria), Am Campus 1, 3400 Klosterneuburg, Austria

[4]Zentrum für Molekularbiologie der Pflanzen, Universität Tübingen, 72076 Tübingen, Germany

[5]Laboratory of Biochemistry, Wageningen University, Dreijenlaan 3, 6703HA Wageningen, the Netherlands

[6]Institute of Experimental Botany, ASCR, Rozvojová 263, 16502 Prague, Czech Republic

[7]Plant Science and Landscape Architecture, University of Maryland, College Park, MD 20742, USA

* Correspondence: eva.benkova@ist.ac.at; Tel +43 2243 9000-5301; Fax +43 2243 9000 2000

Running title: CRFs control *PIN* gene transcription

ABSTRACT

Auxin and cytokinin are key endogenous regulators of plant development. Although cytokinin-mediated modulation of auxin distribution is a developmentally crucial hormonal interaction, its molecular basis is largely unknown. Here we disclose a core mechanistic framework for cytokinin–auxin cross-talk and a direct regulatory link between the cytokinin signaling and the auxin transport machinery. We show that the CYTOKININ RESPONSE FACTORS (CRFs), transcription factors downstream of cytokinin perception, transcriptionally control genes encoding *PIN-FORMED* (*PIN*) auxin transporters at a specific *PIN CYTOKININ RESPONSE ELEMENT* (*PCRE*) domain. Removal of this cis-regulatory element effectively uncouples *PIN* transcription from the CRF-mediated cytokinin regulation and attenuates plant cytokinin sensitivity. Hence, CRFs represent the missing cross-talk components which fine-tune auxin transport capacity downstream of cytokinin signaling to control plant development.

Subject terms: auxin, cytokinin, hormonal cross-talk, lateral root organogenesis

Introduction

The hormones auxin and cytokinin are essential to control plant growth and development including early embryogenesis[1,2] and postembryonic organogenic processes, such as root[3–5] and shoot[6] branching, phyllotaxis[7], shoot[8,9] and root apical meristem activity[10,11], and vasculature development[12,13]. The principal pathways that manage their metabolism, distribution, and perception, and the backbone molecular components have been identified[14–17]. Importantly, a complex network of interactions and feedback circuits interconnects both pathways and determines the final outcome of the individual hormone actions. Well-established are the mutual regulation of metabolic[18] and signaling pathways[2,8], as well as the cytokinin-mediated modulation of auxin transport[10–12]. Cytokinin has been shown to influence cell-to-cell auxin transport by modification of the expression of several auxin transport components and thus to modulate auxin distribution important for root development[10,11,19,20]. Through the cytokinin receptor ARABIDOPSIS HISTIDINE KINASE3 (AHK3) and the downstream signaling components ARABIDOPSIS RESPONSE REGULATOR (ARR1) and ARR12, cytokinin has been shown to activate SHY2/IAA3 (SHY2), a repressor of auxin signaling that negatively regulates the PIN auxin transporters[10]. However, thus far, the components of the transcriptional complex that directly controls *PIN* transcription in response to cytokinin are unknown.

Here, we show that the CYTOKININ RESPONSE FACTORS (CRFs)[21] transcriptionally control *PIN-FORMED* (*PIN*) genes encoding auxin transporters at a specific *PIN CYTOKININ RESPONSE ELEMENT* (*PCRE*) domain. Removal of this cis-regulatory element effectively uncouples *PIN* transcription from the CRF-dependent regulation and attenuates plant cytokinin sensitivity. Accordingly, plants with modified CRF activity exhibit alterations in the expression of *PIN* genes and developmental defects mimicking phenotypes of auxin distribution mutants. We propose that the CRFs act as components of the transcriptional regulatory complex which mediates transcriptional control downstream of cytokinin and fine-tunes *PIN* expression during plant growth and development.

Results

Loss of a PCRE element results in cytokinin-insensitive PIN7 expression To explore the upstream pathway mediating cytokinin-dependent *PIN* transcription, we searched for the

regulatory elements by a promoter deletion analysis in *PIN7* and *PIN1* promoters (Supplementary Fig. 1a). Initially, we focused on *PIN7* of which transcription has previously been shown to be activated by cytokinin[11,12]. We confirmed that the promoter (1,423 bp upstream of the translational start site) of *PIN7* fused to the *green fluorescent protein* (*GFP*) reporter gene (Supplementary Fig.1a) is activated by cytokinin and that this region is sufficient to mediate the hormonal response (Fig. 1a). The abrupt change in the cytokinin response as a consequence of a 200-bp element deletion between 1,423 bp and 1,223 bp upstream of the *ATG* start codon hinted at the presence of a cis-regulatory element required for the cytokinin-mediated transcriptional control of *PIN7* (Fig. 1b). The role of this regulatory element, designated as *PIN CYTOKININ RESPONSE ELEMENT7* (*PCRE7*), in cytokinin-sensitive expression was further tested with a *PIN7-GFP* translational construct driven by the truncated *ΔPIN7* promoter. Quantification of the membrane PIN7-GFP signal demonstrated that the expression, when driven by the truncated promoter, was largely insensitive to cytokinin treatment in the cells of the central root cylinder (Fig. 1c-e), as well as in the initials of lateral root primordia (Supplementary Fig. 2a-e). The *ΔPIN7* promoter activity was significantly weakened in the root provasculature and columella cells when compared to the full *PIN7* promoter, indicating the importance of this promoter element for the regulation of the *PIN7* steady state expression (Fig. 1a and c compared to b, d and e). Hence, the loss of cytokinin sensitivity as a consequence of the promoter truncation implies the presence of a specific cis-regulatory element on which the cytokinin-susceptible transcriptional complex might act to fine-tune *PIN7* expression in response to cytokinin. The severely attenuated expression of the *ΔPIN7* promoter indicates that cytokinin might, through this regulatory element, participate in the establishment and maintenance of the proper expression level of *PIN7*.

Cytokinin insensitive PIN7 transcription modulates plant development. A part of cytokinin-regulated plant growth and development has been proposed to be mediated through cytokinin-controlled *PIN* expression[10,11]. To dissect the developmental role of cytokinin-regulated *PIN* expression, plants expressing *PIN7-GFP* under the control of the truncated cytokinin-insensitive *ΔPIN7* promoter or the wild-type *PIN7* promoter were crossed with the *pin7* mutant background and their seedlings were thoroughly inspected. Root growth analyses revealed that in young seedlings (7 days old), growth of roots expressing either *PIN7::PIN7-GFP/pin7* or

ΔPIN7::PIN7-GFP/pin7 was indistinguishable. In contrast, 14-day-old *ΔPIN7::PIN7-GFP/pin7* roots were significantly longer than control *PIN7::PIN7-GFP/pin7* roots (Fig. 1f and h). Furthermore, attenuation of the cytokinin-mediated *PIN7* transcription strongly interfered with the cytokinin sensitivity of root growth (Fig. 1g and h), root meristem size (Fig. 1i), lateral root initiation and development (Fig. 1g and j). Some phenotype features, such as primary root growth and its resistance to cytokinin, were comparable to the *pin7* phenotype. However, reduced sensitivity of the root meristem as well as of the lateral root initiation to cytokinin were more pronounced in *ΔPIN7::PIN7-GFP/pin7* seedlings.

Altogether these data corroborate the role of the *PCRE7* in fine-tuning *PIN7* expression and show that cytokinin-controlled transcription of *PIN7* through *PCRE7* is critical for proper cytokinin-regulated root growth and development.

Cytokinin response factors (CRFs) control PIN7 transcription. To identify the upstream regulatory factors that control *PIN7* transcription by direct interaction with *PCRE7*, we employed a yeast one-hybrid (Y1H) assay. We screened the REGIA open reading frame (ORF) library that contains a set of ~1,300 *Arabidopsis* transcription factors (TFs) and transcriptional regulators[22]. The Y1H screen with *PCRE7* as bait (Supplementary Fig. 3a), identified CRF2, CRF3, and CRF6 that belong to the cytokinin-inducible subset of the APETALA2/ETHYLENE RESPONSIVE FACTOR family of TFs[21] (Fig. 2a). To confirm that the CRFs physically interact with *PCRE7*, we analyzed the *CRF2::CRF2-GFP* and *35S::CRF6-GFP* transgenic plants through chromatin immunoprecipitation (ChIP) followed by quantitative PCR assays (ChIP-qPCR). Chromatin immunoprecipitated with anti-GFP antibodies was profoundly enriched in the *PCRE7* region. No enrichment was detected when other distant sequences in the *PIN7* (*PIN7* [-553-357]) promoter were tested (Fig. 2c and d; Supplementary Fig. 1c). Hence, CRFs are directly associated with the *PCRE7*.

To gain insight into the role of the CRFs in the regulation of *PIN* transcription, we performed a transient expression assay in *Arabidopsis* protoplasts. The expression of the *PIN7::LUCIFERASE* (*LUC*) reporter was strongly activated when co-expressed with *CRF2* and *CRF6* (Fig. 2e and f), but not with *CRF3* driven by constitutive *35S* promoter (Supplementary Fig. 3b). Noteworthy, when co-expressed, CRF3 significantly attenuated the positive effect of CRF6 on *PIN7::LUC* expression (Supplementary Fig. 3c), indicating that individual CRFs might

regulate *PIN7* transcription differentially. No increase in the *LUC* reporter expression was detected when *CRF2* was co-expressed with the truncated *ΔPIN7::LUC* construct (Fig. 2e). Co-expression with CRF6 stimulated *ΔPIN7::LUC* expression, but less when compared to effect on the *PIN7::LUC* (Fig. 2f) thus further confirming the importance of the *PCRE7* for CRF-dependent transcription. Collectively these data demonstrate that CRFs contribute to the transcriptional control of the *PIN7* gene through physical interaction with a specific domain in its promoter.

CRFs regulate transcription of *PIN1* auxin efflux carrier. Next we examined whether other *PIN* family members are transcriptionally controlled by CRFs similarly to *PIN7*. Using promoter deletion analysis we found that removal of the 200 bp between 1417 bp and 1212 bp upstream of the *ATG* codon resulted in complete cytokinin insensitivity of *PIN1* transcription, hinting at the presence of the *PCRE1* cis-regulatory element mediating cytokinin-induced transcriptional control in the *PIN1* promoter (Supplementary Fig. 1b and 4a-e). A Y1H assay confirmed an interaction of CRF2, CRF3 and CRF6 with this element (Fig. 2b; Supplementary Fig. 3a). Accordingly, chromatin immunoprecipitated with anti-GFP antibodies from *CRF2::CRF2-GFP* and *35S::CRF6-GFP* transgenic plants was profoundly enriched in the *PCRE1*, while no enrichment was detected for distant sequence in the *PIN1* promoter (*PIN1* [-512-433]) (Fig. 2c and d). The expression of *PIN1::LUC*, but not of *ΔPIN1::LUC*, was strongly activated when transiently co-expressed with *CRF2* and *CRF6*, in protoplasts (Fig.2e and f). Similarly to *PIN7*, CRF3 did not significantly affect *PIN1::LUC* expression, but attenuated the *CRF6* stimulatory effect when co-expressed (Supplementary Fig. 3d, e). Altogether, these results indicate that *PIN1* and *PIN7* share common upstream regulatory components controlling their expression in response to cytokinin.

***PCRE1* and *PCRE7* contain motifs recognized by CRFs.** Alignment of *PCRE1* and *PCRE7* elements with the Align program (based on the ClustalW algorithm)[23] displayed a 54% sequence identity, suggesting that the cytokinin-dependent regulation of *PIN1* and *PIN7* might be governed by transcription factors (TFs) recognizing common types of regulatory motifs (Fig. 2h). Previously, the *GCC* box (*AGCCGCC*) has been proposed as a binding motif recognized by ETHYLENE RESPONSE FACTOR1 (ERF1), a TF of the AP2/ERF family [21,24], including

CRF2, CRF3 and CRF4[25]. Scanning of *PIN1* and *PIN7* promoters revealed that neither *PCRE1* nor *PCRE7* contains a *GCC* box, and there is one *GCC* box located at [-483bp] upstream of *ATG* in the *PIN1* promoter (Supplementary Fig. 1d). However, no significant enrichment for the *PIN1* fragment [-512-433] which contains this motif was detected using the ChIP-qPCR assay, indicating that CRF2 and CRF6 do not exhibit an increased affinity to this binding site (Fig. 2c, d). Noteworthy, several studies demonstrated that nucleotides *G2*, *G5*, and *C7* at conserved positions might be essential for the recognition of the *GCC*-derived motif by TFs of the AP2/ERF family[26]. We found that *PCRE1* and *PCRE7* contain *AGCAGAC* and *AGAAGAC* motifs, respectively, with critical nucleotides at conserved positions (Fig. 2h; Supplementary Fig. 1c and d). To examine the relevance of these motifs for CRF binding, we tested whether CRF6 associates with them by ChIP-qPCR. Using specific primer combinations, we inspected enrichment for the short fragments spanning *PCRE1*[27]. Significantly increased enrichment detected for fragments either containing or directly neighboring the *AGCAGAC* site when compared to more distant fragments in *PCRE1*, strongly supports this motif as a CRFs' recognition site (Fig. 2 g). Additional thorough scanning for the presence of *G2*, *G5*, and *C7* motifs revealed one more motif in both *PIN1* as well as *PIN7* promoters (Supplementary Fig.1c and d).

To further support our conclusion on the CRF-mediated regulation of *PIN* expression, we tested whether the *PIN2* promoter, previously found to be cytokinin insensitive[28] might be activated by CRF after introducing the *AGAAGAC* motif. Detailed scanning of the *PIN2* promoter sequence revealed that there are no *AGCAGAC* and *AGAAGAC* motifs present in the *PIN2* promoter sequence within 2500 bp upstream of the translation start and there is one *GCCGTC* motif located at [-698bp] upstream of the translational start. When the *PIN2::LUC* reporter was co-expressed with CRF6, a 1.47±0.38 fold increase of LUCIFERASE activity was detected, indicating modest CRF6 activity for the regulation of *PIN2* promoter (Fig. 2h). Replacement of the *GCCGTC* motif in the *PIN2* promoter by either one or three copies of the *AGAAGAC* motif resulted in a 1.75±0.17 and 3.48±1.02 fold increase of the LUCIFERASE activity, respectively (Fig. 2h). Hence, insertion of a *AGAAGAC* in triplicate into the *PIN2* promoter significantly increased sensitivity to CRF6 (Fig. 2h), thus corroborating relevance of the motif identified in the *PCRE7* element for CRF6-mediated expression. In line with previous observations, no

dramatic effect on *PIN2* as well as on the *PIN2* promoter containing *PCRE7* motifs could be detected when co-expressed with CRF3 (Fig. 2h).

Previously, type-B ARRs have been proposed to mediate cytokinin regulation of *PIN1* and *PIN7* expression through direct transcriptional control of the *IAA3/SHY2* repressor of auxin signaling[10]. Three type-B ARRs (ARR10, ARR11 and ARR14) tested in a Y1H assay did not exhibit interaction with either *PCRE1* or *PCRE7*, which indicates that cytokinin transcriptional regulation of *PIN1* and *PIN7* might not occur through their direct binding to *PCREs* (Supplementary Fig. 3f).

Altogether, these data suggest that CRF2 and CRF6 might recognize specific motifs within *PCRE1* and *PCRE7* with *G2*, *G5*, and *C7* at conserved positions to control *PIN1* and *PIN7* expression

Expression of *PIN7* and *PIN1* is altered in *crf* mutants. The initial expression analysis revealed that the expression patterns of *CRFs* and *PIN1* and *PIN7* largely overlap in roots[29] (Supplementary Fig. 5 compared to Fig. 1a and Supplementary Fig. 4a, c), supporting their role as direct transcriptional regulators. To evaluate the impact of CRFs on *PIN7* and *PIN1* expression in planta, we examined lines with a modulated activity of CRFs (Supplementary Fig. 6). Analyses of *PIN7* expression using qRT-PCR as well as monitoring of *PIN7::PIN7-GFP*, *PIN7::GUS*, *PIN7::GFP* and *PIN7::PIN7-GUS* reporters revealed a significant increase of *PIN7* expression in the root provasculature of *RPS::CRF2* and *35S::CRF6*, but not of *35S::CRF3* lines (Fig. 3a,b,e and Supplementary Fig. 7a-j). This is largely in agreement with the results of a transient protoplast assay (Fig. 2e and f compared to Fig. 3a-c). Lack of the *PCRE7* in the *ΔPIN7::PIN7-GFP* line interfered with the stimulatory effect of CRF2 on *PIN7-GFP* expression, regardless of cytokinin levels (Fig. 3c and d). Analysis of *PIN7* expression using *PIN7::PIN7-GFP*, and *PIN7::GUS* reporters as well as qRT-PCR in mutants lacking either of CRFs revealed attenuated *PIN7* expression in *crf3* and enhanced *PIN7* expression in *crf6* roots (Supplementary Fig. 7 k-t).

Similarly to *PIN7*, *PIN1* expression was significantly upregulated in roots overexpressing *CRF2* as detected using *PIN1::PIN1-GFP* and *PIN1::GFP* reporters as well as by qRT-PCR approach. Deletion of the *PCRE1* in the *ΔPIN1::PIN1-GFP* line interfered with the stimulatory

effect of CRF2 on *PIN1* expression in agreement with the proposed role of the *PCRE1* in CRF-dependent transcriptional control (Supplementary Fig. 8a-d).

Inspection of *crf* loss-of-function mutants further confirmed the role of CRFs in the regulation of *PIN1* expression in planta. *PIN1* expression was significantly reduced in *crf2*, *crf3*, *crf3crf6* and *crf2crf3crf6* loss-of-function mutants (Supplementary Fig. 8d-g), thus resembling the *PIN7* expression pattern in these mutant backgrounds.

Altogether, the expression analysis data support a role of the CRFs in balancing the *PIN7* and *PIN1* transcription. Nevertheless, inconsistency in *PIN7* and *PIN1* expression patterns observed in lines with modulated *CRF* expression, such as downregulation of both *PIN1* and *PIN7* in *crf3*, and upregulation in *crf6*, might reflect the presence of intricate in planta regulatory mechanisms, e.g. the existence of a transcriptional complex in which additional components could function as modifiers. This is strongly supported by recent observations that individual CRFs might interact with other family members, as well as with type-B ARRs[30]. Collectively, our data demonstrate that CRFs contribute to balancing *PIN7* and *PIN1* expression and that CRF homologs might have specific functions in the control of *PIN* expression.

CRFs mutants exhibit an auxin transport-defective phenotype. To examine a role of CRFs as direct upstream regulators of *PIN* transcription, we analyzed in detail the phenotype of plants with modulated *CRF* expression. Altered expression of *PINs* in *crf* loss-of-function mutants might result in an abnormal auxin distribution and, consequently, in developmental and patterning defects as previously demonstrated for auxin distribution mutants[1,31]. Indeed, auxin measurements in root tips of *crf3crf6* mutants revealed an increase in auxin levels (Fig. 4a). Similarly, the auxin accumulation at root tips of a mutant lacking PIN4 auxin efflux carrier activity has been previously observed[31].

By closer examination of plants lacking CRF activity, developmental abnormalities were found reminiscent of those caused by impaired auxin transport. A significantly enhanced number of embryonic defects, such as abnormal divisions of upper suspensor cells and in the embryo proper, and occasionally the appearance of double embryos, was observed in embryos of *crf2*, *crf3* and *crf3crf6* loss-of-function mutants when compared with control lines (Fig. 4b-i), thus phenocopying the *pin1*, *pin7*, and multiple *pin* embryo defects[1]. Accordingly, *CRF2*, *CRF3*, and *CRF6* expression was detected in early embryos (Supplementary Fig. 5). Lack of functional

CRF2, CRF3, both CRF3 and CRF6 or CRF2, CRF3, CRF6 correlated with reductions in root length, root meristem size, and lateral root initiation (Fig. 4j-n), which are developmental aberrations typically associated with defective auxin transport[3,32,33]. On the contrary, *crf6* loss-of-function mutants, in which *PIN7* expression was enhanced, exhibited longer roots and a larger root meristem (Fig. 4j-n). Altogether, modulation of CRF activity alters auxin accumulation in the root tips, and leads to developmental defects in many aspects, mimicking phenotypes of auxin distribution mutants[1,31,32].

CRFs fine-tune root system response to cytokinin and auxin. Typically, an increase in cytokinin activity alters root growth and development: cytokinins restrict root elongation growth, cause shortening of the root meristem size, and compromise the initiation and development of the lateral roots[4,5,10,11,34,35]. Whereas cytokinin inhibitory effects of root elongation involves ethylene[11,34], reduction of the root meristem size, as well as lateral root initiation by cytokinin occurs largely in an ethylene independent manner[5,11]. To examine the possible role of CRFs in cytokinin-mediated root system establishment, lines with modulated CRF activity were exposed to increased cytokinin concentrations. We found that neither gain nor loss of CRF activity dramatically changed root growth response to cytokinin (Fig. 4l and o). The root meristem cytokinin response was unaffected in *crf2* and *crf6* mutants and reduced in *crf3* and *crf3crf6* as well as *crf2crf3crf6* mutants (Fig. 4m). Constitutive expression of *CRF2*, *CRF3*, and *CRF6* reduced root meristem response to cytokinin (Fig. 4p). Noteworthy, most pronounced changes were observed in cytokinin effect on lateral root initiation and development. The significant increase in cytokinin inhibitory effects on both lateral root initiation and development was detected in *crf3, crf3crf6* and *crf2crf3crf6* mutants (Fig. 4n; Supplementary Fig. 9a-e), whereas *CRF2* and *CRF6* overexpression attenuated cytokinin effects (Fig. 4r; Supplementary Fig. 9f, g). In contrast to cytokinin, root system response to auxin was reduced in *crf3*, *crf3crf6* and *crf3crf3crf6* mutants, which was manifested by an attenuated stimulatory effect of auxin on lateral root initiation (Supplementary Fig. 10a-e). Constitutive expression of *CRF2* led to significantly enhanced response to auxin whereas no dramatic changes in lateral root initiation after auxin treatment in either the *CRF3* or *CRF6* overexpressor line when compared to wilde type control were detected (Supplementary Fig. 10f-h). Hence, perturbations in *CRF* expression

affect root response to cytokinin and auxin, and indicate that CRFs through control of auxin transport might fine-tune cytokinin- and auxin-mediated root growth and development.

Discussion

Auxin gradients represent universal mechanisms to control plant organogenesis. Modulation of the activity of the transport machinery that regulates auxin distribution directly impacts on organ formation and patterning and, thus, accounts for a developmentally efficient tool to flexibly adapt plant architecture depending on the changing environmental conditions. Recently, evidence accumulates that exogenous factors, such as light or gravity, through their endogenous counterpart, i.e. plant hormones including ethylene, gibberellin, jasmonate and cytokinin, modulate the activity of the polar auxin transport machinery to direct plant growth and development[10,11,19,36–39]. However, the molecular bases of these regulations are scarcely understood so far.

Here we demonstrate that the expression of auxin efflux transporters can be effectively uncoupled from the cytokinin control through deletion of the *PCRE* cis-regulatory element in the promoter of the *PIN* auxin efflux carrier gene. The loss of cytokinin-dependent *PIN7* transcription impacts on the cytokinin-mediated root growth and branching, thus supporting the developmental significance of the tightly cytokinin-controlled PIN-dependent auxin transport in the establishment of the root system architecture.

Attempts to reveal components of the upstream regulatory pathway acting at the *PCRE* led to the identification of CRFs as direct transcriptional regulators. Originally, CRFs have been found as a subgroup of the APETALA 2 (AP2) family of TFs, which are rapidly induced by cytokinin, and they have been proposed to mediate the transcriptional response to cytokinin[21]. However, the CRFs' downstream targets and pathways remained unknown so far. Here, we show that through interaction with the cis-regulatory *PCRE*, presumably through recognition of the *AGCAGAC*-like motif, CRFs control expression of *PIN1* and *PIN7*.

Modulation of the CRF activity results in significant changes of the *PIN1* and *PIN7* expression patterns and in phenotype aberrations reminiscent of mutants with defective auxin transport[1,31,32]. This, together with a significant overlap in the expression of *PIN* and *CRF* genes during embryogenesis, in the root meristems and lateral root primordia, strongly supports a role of CRFs in the regulation of *PIN* expression. Accordingly, the expression of several *CRFs* in

vascular tissue has been correlated with alterations of the vascular patterning in CRF loss-of-function mutants[38], similarly to those observed in auxin transport mutants[39].

In this light, the identification of the *PIN* genes as direct targets of CRFs reveals a missing direct regulatory link between the cytokinin signaling and the auxin transport machinery. Moreover, *CRF2* (*TARGET OF MONOPTEROS* [*TMO3*]) as a direct transcriptional target of the *AUXIN RESPONSE FACTOR5*/*MONOPTEROS*[42] might account for an important convergence point to the previously characterized *AHK3-ARR*, *ARR12-IAA3*/*SHY2* regulatory chain[10] and balance both auxin and cytokinin input to control auxin transport. Furthermore, the recent observation that *CRF6* is induced by numerous stresses[29] hints at a role of CRFs as factors modulating auxin transport in response to environmental signals.

METHODS

Plant material and growth conditions. The transgenic *Arabidopsis thaliana* (L.) Heynh. lines have been described elsewhere: *PIN1::PIN1-GFP*[3], *pin7-2*[3], *PIN7::PIN7-GFP*[32], *PIN7::GUS*[1], *RPS5A::CRF2*[42], *35S::EGFP- CRF6*[43]. The previously characterized CRF knockout mutants[21] were obtained from various T-DNA insertion mutant seed collections: *crf2-1*, *crf2-2*, *crf3-1 and crf3-2* from the Salk Institute Genomic Analysis Laboratory (SAIL, former GARLIC) T-DNA insertion lines from the Torrey Mesa Research Institute[44] and *crf6-S2 and crf6-11.2* from GABI-Kat[45]. The *crf3crf6* double and *crf2crf3crf6* triple mutants were generated from *crf3-1* and *crf6-S2* and *crf2-2*, *crf3-1* and *crf6-S2* respectively. Primers and T-DNA accession numbers are listed in Supplementary Table 2. Seeds of *Arabidopsis* (accession Columbia-0) were plated and grown on square plates with solid half-strength Murashige and Skoog (MS) medium supplemented with 0.5 g/L MES, 10 g/L Suc, and 0.8% agar. The plates were incubated at 4°C for 48 h to synchronize seed germination and then grown vertically in growth chambers under a 16-h/8-h day/night cycle photoperiod at 18°C.

Cloning and generation of transgenic lines. For promoter analysis of *PIN1* and *PIN7*, particular promoter fragments were amplified by PCR and cloned into the *pGEM-T* vector. The used primers contained unique restriction sites: PstI-sense and BamHI-antisense for PIN1 and SalI-sense and BamHI-antisense for *PIN7*, allowing digestion and subsequent cloning into the *pGREEN* binary vector. The resulting constructs contained transcriptional fusions between the

PIN1 or *PIN7* promoter variants and the enhanced green fluorescent protein (EGFP) with a nuclear localization signal (NLS). Primers used for cloning are listed in Supplementary Table 1. The translational fusion Δ*PIN1::PIN1-GFP* was obtained by modifying *PIN1::PIN1-GFP* (in *pBINPLUS* vector backbone[3]) as follows: the *PIN1* promoter sequence from -258 to -2320 relative to the initiating *ATG* was removed by XbaI digestion and replaced by the *PIN1* promoter sequence spanning the -258 to -1212 region. Δ*PIN7::PIN7-GFP* was derived from *PIN7::PIN7-GFP* in *pBINPLUS*[1] by removal of the EcoRI fragment. The truncated promoter construct contained 1141 bp upstream of the translational start site. Expression plasmids were generated by standard molecular biology protocols and Gateway technology (Invitrogen). ORFs were amplified from a cDNA template with Pfu DNA Polymerase (Promega) and fused to the Gateway attB sites by PCR. *pDONR221* and p4-p1r were used as ENTRY vectors. The structure and sequence of all destination vectors were as described[46,47] and are available online at http://www.psb.ugent.be/gateway/ or otherwise referenced. *35S::CRF3* and *35S::CRF6* were obtained by cloning the ORFs of *CRF3* and of *CRF6* into destination vectors *pK7WG2.0* and *pK7WG2D*, respectively. Overexpression of these lines was confirmed by qPCR, primers are included in Supplementary Table 1. The *CRF3* and *CRF6* (2-kb) promoters were cloned in *pMK7S*NFm14GW*, generating the *ProCRF3:NLS-GFP-GUS* and *ProCRF6:NLS-GFP- GUS* constructs (transcriptional fusions between the promoters and the gene encoding the EGFP-GUS fusion protein), respectively. The *CRF2::CRF2-GFP* fusion, used for the ChIP experiments, is a *CRF2* promoter fragment (2 kb upstream of the coding sequence of *CRF2*) cloned into the *PgreenIIK* vector, resulting in a fusion with the NLS and EGFP. All transgenic plants were generated by the floral dip method[48]. At least two independent transgenic lines were examined for expression pattern.

Quantitative RT-PCR. RNA was extracted with the RNeasy kit (Qiagen) from excised root tips of 7-day-old root sample. A DNase treatment with the RNase-free DNase Set (Qiagen) was carried out for 15 minutes at 25°C. Poly(dT) cDNA was prepared from 1 µg of total RNA with the iScript™cDNA Synthesis Kit (Biorad) and analyzed on a LightCycler 480 (Roche Diagnostics) with the SYBR GREEN I Master kit (Roche Diagnostics) according to the manufacturer's instructions. Targets were quantified with specific primer pairs designed with the Beacon Designer 4.0 (Premier Biosoft International, Palo Alto, CA). All PCRs were performed

in triplicate. Expression levels were first normalized to ACTIN2 expression levels and then to the respective expression levels in the wild type. The primers used to quantify gene expression levels are listed in Supplementary Table 1.

Phenotypic analysis. For the phenotypic analysis of the root parameters (root length and root meristem size) and the lateral root primordia development, 10-20 seedlings of 7- and 10-day-old seedlings were processed as described[49]. The cytokinin concentrations were adapted to the experimental set up. Typically, to examine root growth response to cytokinin, low 0.25, 0.5 and 0.1 μM cytokinin concentrations were applied. The cytokinin impact on PIN expression was examined 8 hours after treatment with cytokinin, therefore higher 2 and 5 μM concentrations were applied. For the analysis of the root growth kinetics, seedlings were recorded every day for 14 days with an EOS035 Canon Rebel Xti camera. Long-term root growth observations for 28 days were performed on Petri dishes of 245 per 245 mm size. All data were analyzed with the ImageJ software (NIH; http://rsb.info.nih.gov/ij) as described[11].

Histochemical and histological analysis. Seedlings were stained to detect *GUS* expression and cleared as previously described[49]. All samples were analyzed by differential interference contrast microscopy (Olympus BX51). Embryos were labelled by immunofluorescence as described[50]. Primary rabbit anti-GFP and rabbit anti-PIN1 antibodies were diluted 1:600 and 1:400, respectively, and secondary anti-rabbit-Alexa 488 and anti-rabbit Alexa 546 antibodies were diluted 1:600 in 3% bovine serum albumin (BSA) in phosphate buffered saline. Whole-mount root immunolocalization was performed using an automated system (Intavis in situ pro) as previously described[50] using anti-PIN1 antibody diluted 1:1000 and CY3-conjugated anti-rabbit antibody (Sigma) diluted 1:600. Live-imaging was done with a confocal laser scanning microscopy (LSM 510, Zeiss). Images were analyzed with the LSM Image Browser (Zeiss).

Confocal imaging and image analysis. Confocal microscopy images were obtained with the Zeiss LSM 510, Zeiss LSM 710, or Olympus FV10 ASW confocal scanning microscopes using either 20x or 60x (water immersion) objectives. Fluorescence signals were detected for GFP (excitation 488 nm and emission 507 nm) and propidium iodide (excitation 536 nm and emission 617 nm). Development of lateral root primordia was followed in real time as described[19]. To

evaluate relative *PIN* expression levels, the GFP signal in root meristems was measured on membranes of pericycle and endodermal cells adjacent to the quiescent center. Fluorescence intensities of the PIN-GFP membrane signals were quantified with ImageJ (NIH; http://rsb.info.nih.gov/ij) as described[51]. 10-15 seedlings were used for analysis. The statistical significance was evaluated with the Student's t-test.

Auxin accumulation in the root tip of *crf3crf6* double mutants. Root tips (2-mm segments, about 100 mg) of 6-day-old *Arabidopsis thaliana* (L.) Heynh. seedlings grown on vertical plates were separated and collected in 300 µl Bieleskis solution and homogenized. After overnight extraction at -20°C, the tissues were separated by centrifugation (15,000 g) and extracts were evaporated to dryness. Free IAA determination was done as described[52].

Yeast one-hybrid screen. The yeast strain YM4271 and destination vectors *pDEST-MW1* and *pDEST- MW2* have been previously described[53]. Yeast reporter strains were designed as described[53]. For the Y1H cDNA library screen, the 200-bp promoter fragments *PCRE1* and *PCRE7* were cloned into the destination vectors *pDEST-MW1* and *pDEST- MW2*, respectively, by Gateway cloning (for primers sequences see Supplementary Table 1). The DNA baits were integrated into yeast using the high efficiency transformation protocol according to the Yeast Protocol Handbook (Clontech) except that 1 µg of linearized plasmid DNA was added to the competent yeast, the heat shock period at 42°C was extended to 20 min and the cells were resuspended in 150 µl TE buffer. The cDNA Y1H library screen was performed with a REGIA and REGULATORS (RR) collection, previously described[22]. For the transformation of one TF, 20 µl of competent yeast, 2 µl of carrier DNA, 100 ng plasmid (TF) DNA and 100 µl of TE/LiAC/PEG were used. Yeast cells were resuspended in 20 µl TE buffer and spotted on SD-His-Ura-Trp medium. After 3 days of growing, replica plates were made with 0, 15 and 30 mM 3-aminotriazole and positive clones were selected after 6 to 8 days of incubation at 30°C.

Transient expression in *Arabidopsis* mesophyll protoplasts. Mesophyll protoplasts were isolated from rosette leaves of 4-week-old *Arabidopsis* plants grown in soil under controlled environmental conditions in a 16-h/8-h light/dark cycle or under continuous light at 21°C. Protoplasts were isolated and transient expression assays were carried out as described[54] with

modifications[55]. Protoplasts were co-transfected with 20 µg of a reporter plasmid that contained *fLUC*, a reporter gene driven by the corresponding promoter, 2 µg of normalization plasmid expressing the *Renilla luciferase* (*rLUC*) under the control of the *35S* promoter, and 20 µg of the effector construct. For the reporter constructs, the *pEN-L4-Pro-R1* vector (with Pro representing *PIN1:LUC*, Δ*PIN1::LUC*, *PIN7::LUC*, and Δ*PIN7::LUC*) was recombined together with *pEN-L1-fLUC-L2* by Multisite Gateway LR cloning with *pm42GW736*. For the effector constructs, the *pEN-L1-ORF-R2* plasmids (with the ORF of *CRF2*, *CRF3*, or *CRF6*) were used to introduce the ORFs by Gateway LR cloning into *p2GW7* for overexpression.

The total amount of DNA was equalized in each experiment with the *p2GW7-GUS* mock effector plasmid. After transfection, protoplasts were incubated overnight and then lyzed; *fLUC* and *rLUC* activities were determined with the Dual-Luciferase reporter assay system (Promega). Variations in transfection efficiency and technical errors were corrected by normalization of fLUC by the rLUC activities. The mean value was calculated from three measurements and each experiment was repeated at least three times.

Transient expression in *Arabidopsis* root suspension culture protoplasts.

The luciferase assays were performed from 3-days old *Arabidopsis* root suspension culture by PEG mediated transformation. Protoplasts were isolated in enzyme solution (1% cellulose;Yakult, 0.2% Macerozyme ;Yakult in B5-0.34M glucose-mannitol solution; 2.2 g MS with vitamins, 15.25 g glucose, 15.25 g mannitol, H2O to 500 mL pH to 5.5 with KOH) with slight shaking for 3-4 hours, centrifuged at 800g for 5 minutes. The pellet was washed with B5-0.34M glucose mannitol solution and resuspended in B5-0.34M glucose mannitol solution to a final concentration of 2 x105 per 50 µL. 2µg of reporter and effector plasmid DNAs were gently mixed together with 50 µL of protoplast suspension and 60 µL of PEG solution (0.1 M Ca(NO3)2, 0.45 M Mannitol, 25% PEG 6000) and incubated in the dark for 10 minutes. Then 140 µL of 0.275M Ca(NO3)2 solution was added to wash off PEG, centrifugad at 800g for 5 minutes and supernatant was removed. The protoplast pellet was resuspended in 200 µL of B5-0.34M glucose mannitol solution and incubated for 16h in the dark at room temperature. The luciferase assays were performed using a Dual-Luciferase® Reporter Assay System (Promega, Madison, WI, USA) as described for mesophyll protoplasts above. For cloning of the *PIN2wt:LUC* construct, 1.5kb fragment of the *PIN2* promoter upstream from the translational

start was PCR amplified from the genomic DNA using SalI-Fw and NcoI-Rv primers and the PCR product was subsequently cloned as SalI+NcoI fragment into the pGreen008-II-Luc vector[56] in frame with the coding sequence of the *LUC* gene.

For introducing *PCRE7* motives mutagenesis by PCR-driven overlap extension technique was used as described previously in[57]. Briefly, intermediate primers containing PCRE7 motives were designed with complementary ends and PCRs were performed using following primer combinations (listed in Supplementary Table1): For introducing *PCRE7-1* motif, SalI-Fw primer in combination with PCRE7-1-Rv and NcoI-Rv primer in combination with *PCRE7-1*-Fw were used and *PIN2wt* promoter DNA was used as template. The two PCRs products were purified and combined in equal concentrations and were subsequently used as template in the extension PCR round to get a full length *PIN2* promoter with *PCRE7-1* motif. Similarly for introducing *PCRE7-3,* SalI-Fw primer in combination with PCRE7-3-Rv and NcoI-Rv primer in combination with PCRE7-3-Fw were used, in this case and *PIN2* promoter with *PCRE7-1* motif was used as template. The two PCRs products were purified and combined in equal concentrations and were subsequently used as template in the extension PCR round to get a full length *PIN2* promoter with *PCRE7-3* motif. The PCR products were subsequently cloned into as SalI+NcoI fragment into the *pGreen008-II-Luc* vector.

Chromatin immunoprecipitation assay. ChIP experiments were done as described[58] with minor modifications. One gram of tissue from 8-day-old plants was harvested and immersed in 1% formaldehyde under vacuum for 10 min. Glycine was added to a final concentration of 0.125 M and incubation was continued for 5 min. After washing, the nuclei were isolated and cross-linked DNA/protein complexes were fragmented by sonication with a Bioruptor sonicator (Diagenode), resulting in fragments of approximately 500 bp. After centrifugation (at 500 g), the supernatant was precleared with 80 µl of sheared salmon sperm DNA and protein A agarose (Millipore), of which 10 µl was used as input and the remainder was divided into three samples. To two samples (IP1 and IP2), 25µl GFP-Trap®_A coupled to agarose beads (Chromotec) was added, whereas to the third sample, which served as IgG control, an equal volume of nonspecific control serum was added, consisting of sonicated salmon sperm DNA, BSA, and Protein A (Salmon Sperm DNA/Protein-A agarose-50% slurry; Millipore). The samples were incubated overnight and immunoprecipitates were subsequently eluted from the beads. All centrifugation

steps with bead-containing samples were done at 500 g. Proteins were de-cross-linked and DNA was purified by phenol/chloroform/isoamyl alcohol extraction and ethanol precipitation. Pellets were resuspended in MiliQ water. The concentration of ChIP DNA was measured with the Quant-iT double-stranded DNA HS assay kit (Invitrogen). The SYBR Green I Master kit (Roche Diagnostics) was used for all quantitative PCRs. *ACTIN2* and promoter regions of *PIN1* (433-512 bp upstream of the start codon) and *PIN7* (357-553 upstream of the ATG) were utilized as negative controls. All primer sequences, including those for *PCRE1* and *PCRE7*, as well as primers used for identification of CRF motif are listed in Supplementary Table 1. To analyze the ChIP enrichment from quantitative PCR data, the Percent Input Method and Fold Enrichment Method were used.

Each ChIP DNA fractions' Ct value was normalized to the Input DNA fraction Ct value for the same qPCR Assay (ΔCt). ΔCt [normalized ChIP] = (Ct [ChIP] - (Ct [Input] - Log2 (Input Dilution Factor))). In which Input Dilution Factor (Fd) = 1/100 (fraction of the input chromatin saved). The average of normalized ChIP Ct values for replicate samples was calculated. Percent input was then calculated as: % Input = 2 (-ΔCt [normalized ChIP]). The normalized ChIP fraction Ct value was adjusted for the normalized background (IgG) fraction Ct value (first ΔΔCt). ΔΔCt [ChIP/IgG] = ΔCt [normalized ChIP] - ΔCt [normalized IgG]. IP Fold Enrichment above the sample specific background was calculated as linear conversion of the first ΔΔCt: Fold Enrichment = 2(-ΔΔCt [ChIP/IgG]). Standard deviations were calculated for IP1 and IP2 as ln(2)*dSD*FC and for IgG as ln(2)*dSD, with FC the fold change. ChIP data were obtained from single experiments, but similar data were acquired from three independent experiments.

ACKNOWLEDGMENTS

We thank Dr. L. De Veylder for sharing yeast strain and vectors, Prof. J. Kieber and Dr. A. Rashotte for sharing material, Dr. B. Berckmans, F. De Winter, Dr. B. Parizot for technical advice and Dr. A. Bleys for help in preparing the manuscript. This work was supported by the European Research Council Starting Independent Research grant (ERC-2007-Stg-207362-HCPO to E.B, M.S, C.C), by the Ghent University Multidisciplinary Research Partnership "Biotechnology for a Sustainable Economy" no.01MRB510W, by the Research Foundation - Flanders (grant 3G033711 to J.A.O.), and by the Interuniversity Attraction Poles Programme (IUAP P7/29 "MARS") initiated by the Belgian Science Policy Office. I.D.C. and S.V. are post-doctoral fellows of the Research Foundation - Flanders (FWO).

REFERENCES

1. Friml, J. *et al.* Efflux-dependent auxin gradients establish the apical-basal axis of Arabidopsis. *Nature* **426,** 147–153 (2003).

2. Müller, B. & Sheen, J. Cytokinin and auxin interaction in root stem-cell specification during early embryogenesis. *Nature* **453,** 1094–1097 (2008).

3. Benková, E. *et al.* Local, efflux-dependent auxin gradients as a common module for plant organ formation. *Cell* **115,** 591–602 (2003).

4. Bielach, A. *et al.* Spatiotemporal regulation of lateral root organogenesis in Arabidopsis by cytokinin. *Plant Cell* **24,** 3967–81 (2012).

5. Laplaze, L. *et al.* Cytokinins act directly on lateral root founder cells to inhibit root initiation. *Plant Cell* **19,** 3889–3900 (2007).

6. Leyser, O. The control of shoot branching: an example of plant information processing. *Plant Cell Env.* **32,** 694–703 (2009).

7. Reinhardt, D. *et al.* Regulation of phyllotaxis by polar auxin transport. *Nature* **426,** 255–260 (2003).

8. Zhao, Z. *et al.* Hormonal control of the shoot stem-cell niche. *Nature* **465,** 1089–1092 (2010).

9. Yoshida, S., Mandel, T. & Kuhlemeier, C. Stem cell activation by light guides plant organogenesis. *Genes Dev* **25,** 1439–1450 (2011).

10. Dello Ioio, R. *et al.* A genetic framework for the control of cell division and differentiation in the root meristem. *Science (80-.).* **322,** 1380–1384 (2008).

11. Růžička, K. *et al.* Cytokinin regulates root meristem activity via modulation of the polar auxin transport. *Proc Natl Acad Sci USA* **106,** 4284–4289 (2009).

12. Bishopp, A. *et al.* A mutually inhibitory interaction between auxin and cytokinin specifies vascular pattern in roots. *Curr. Biol.* **21,** 917–26 (2011).

13. Hejátko, J. *et al.* The histidine kinases CYTOKININ-INDEPENDENT1 and ARABIDOPSIS HISTIDINE KINASE2 and 3 regulate vascular tissue development in Arabidopsis shoots. *Plant Cell* **21,** 2008–2021 (2009).

14. Dharmasiri, N. *et al.* Plant development is regulated by a family of auxin receptor F box proteins. *Dev Cell* **9,** 109–119 (2005).

15. Hwang, I. & Sheen, J. Two-component circuitry in Arabidopsis cytokinin signal transduction. *Nature* **413,** 383–389 (2001).

16. Inoue, T., Higuchi, M., Hashimoto, Y. & Seki, M. Identification of CRE1 as a cytokinin receptor from Arabidopsis. *Nature* **409,** 48–51 (2001).

17. Kepinski, S. & Leyser, O. The Arabidopsis F-box protein TIR1 is an auxin receptor. *Nature* **435,** 446–451 (2005).

18. Jones, B. *et al.* Cytokinin regulation of auxin synthesis in Arabidopsis involves a homeostatic feedback loop regulated via auxin and cytokinin signal transduction. *Plant Cell* **22,** 2956–69 (2010).

19. Marhavý, P. *et al.* Cytokinin modulates endocytic trafficking of PIN1 auxin efflux carrier to control plant organogenesis. *Dev Cell* **21,** 796–804 (2011).

20. Pernisová, M. *et al.* Cytokinins modulate auxin-induced organogenesis in plants via regulation of the auxin efflux. *Proc Natl Acad Sci USA* **106,** 3609–3614 (2009).

21. Rashotte, A. M. *et al.* A subset of Arabidopsis AP2 transcription factors mediates cytokinin responses in concert with a two-component pathway. *Proc Natl Acad Sci USA* **103,** 11081–11085 (2006).

22. Castrillo, G. *et al.* Speeding cis-trans regulation discovery by phylogenomic analyses coupled with screenings of an arrayed library of Arabidopsis transcription factors. *PLoS One* **6,** e21524 (2011).

23. Lu, G. & Moriyama, E. N. Vector NTI, a balanced all-in-one sequence analysis suite. *Briefings Bioinforma.* **5 ,** 378–388 (2004).

24. Fujimoto, S. Y., Ohta, M., Usui, a, Shinshi, H. & Ohme-Takagi, M. Arabidopsis ethylene-responsive element binding factors act as transcriptional activators or repressors of GCC box-mediated gene expression. *Plant Cell* **12,** 393–404 (2000).

25. Weirauch, M. T. *et al.* Determination and Inference of Eukaryotic Transcription Factor Sequence Specificity. *Cell* **158,** 1431–1443 (2015).

26. Hao, D., Yamasaki, K., Sarai, A. & Ohme-Takagi, M. Determinants in the Sequence Specific Binding of Two Plant Transcription Factors, CBF1 and NtERF2, to the DRE and GCC Motifs†. *Biochemistry* **41,** 4202–4208 (2002).

27. Hall, D. B., Wade, J. T. & Struhl, K. An HMG Protein , Hmo1 , Associates with Promoters of Many Ribosomal Protein Genes and throughout the rRNA Gene Locus in Saccharomyces cerevisiae †. **26,** 3672–3679 (2006).

28. Růžička, K. *et al.* Arabidopsis PIS1 encodes the ABCG37 transporter of auxinic compounds including the auxin precursor indole-3-butyric acid. *Proc. Natl. Acad. Sci. U. S. A.* **107,** 10749–53 (2010).

29. Zwack, P., Robinson, B., Risley, M. & Rashotte, A. Cytokinin Response Factor 6 Negatively Regulates Leaf Senescence and is Induced in Response to Cytokinin and Numerous Abiotic Stresses. *Plant Cell Physiol* (2013).

30. Cutcliffe, J. W., Hellmann, E., Heyl, A. & Rashotte, A. M. CRFs form protein-protein interactions with each other and with members of the cytokinin signalling pathway in Arabidopsis via the CRF domain. *J Exp Bot* **62,** 4995–5002 (2011).

31. Friml, J. *et al.* AtPIN4 mediates sink-driven auxin gradients and root patterning in Arabidopsis. *Cell* **108,** 661–673 (2002).

32. Blilou, I. *et al.* The PIN auxin efflux facilitator network controls growth and patterning in Arabidopsis roots. *Nature* **433,** 39–44 (2005).

33. Laskowski, M. *et al.* Root system architecture from coupling cell shape to auxin transport. *PLoS Biol.* **6,** e307 (2008).

34. Cary, A. J., Liu, W. & Howell, S. H. Cytokinin action is coupled to ethylene in its effects on the inhibition of root and hypocotyl elongation in Arabidopsis thaliana seedlings. *Plant Physiol.* **107,** 1075–1082 (1995).

35. Dello Ioio, R. *et al.* Cytokinins determine Arabidopsis root-meristem size by controlling cell differentiation. *Curr. Biol.* **17,** 678–82 (2007).

36. Abas, L. *et al.* Intracellular trafficking and proteolysis of the Arabidopsis auxin-efflux facilitator PIN2 are involved in root gravitropism. *Nat Cell Biol* **8,** 249–256 (2006).

37. Ding, Z. *et al.* Light-mediated polarization of the PIN3 auxin transporter for the phototropic response in Arabidopsis. *Nat Cell Biol* **13,** 447–452 (2011).

38. Swarup, R. *et al.* Ethylene upregulates auxin biosynthesis in Arabidopsis seedlings to enhance inhibition of root cell elongation. *Plant Cell* **19,** 2186–2196 (2007).

39. Willige, B. C., Isono, E., Richter, R., Zourelidou, M. & Schwechheimer, C. Gibberellin regulates PIN-FORMED abundance and is required for auxin transport-dependent growth and development in Arabidopsis thaliana. *Plant Methods* **23,** 2184–2195 (2011).

40. Zwack, P. J. *et al.* Vascular expression and C-terminal sequence divergence of cytokinin response factors in flowering plants. *Plant Cell Physiol.* **53,** 1683–95 (2012).

41. Scarpella, E., Marcos, D., Friml, J. & Berleth, T. Control of leaf vascular patterning by polar auxin transport. *Genes Dev.* **20,** 1015–1027 (2006).

42. Schlereth, A. *et al.* MONOPTEROS controls embryonic root initiation by regulating a mobile transcription factor. *Nature* **464,** 913–916 (2010).

43. Inzé, A. *et al.* A subcellular localization compendium of hydrogen peroxide-induced proteins. *Plant Cell Env.* **35,** 308–320 (2012).

44. Sessions, A. *et al.* A high-throughput Arabidopsis reverse genetics system. *Plant Cell* **14,** 2985–2994 (2002).

45. Rosso, M. G. *et al.* An Arabidopsis thaliana T-DNA mutagenized population (GABI-Kat) for flanking sequence tag-based reverse genetics. *Plant Mol Biol* **53,** 247–259 (2003).

46. Karimi, M., Inzé, D. & Depicker, A. GatewayTM vectors for Agrobacterium-mediated plant transformation. *Trends Plant Sci.* **7,** 193–195 (2002).

47. Karimi, M., Depicker, A. & Hilson, P. Recombinational cloning with plant gateway vectors. *Plant Physiol.* **145,** 1144–1154 (2007).

48. Clough, S. J. & Bent, A. F. Floral dip: a simplified method for Agrobacterium-mediated transformation of Arabidopsis thaliana. *Plant J.* **16,** 735–743 (1998).

49. Malamy, J. E. & Benfey, P. N. Organisation and cell differentiation in lateral roots of Arabidopsis thaliana. *Development* **124,** 33–44 (1997).

50. Sauer, M., Paciorek, T., Benková, E. & Friml, J. Immunocytochemical techniques for whole-mount in situ protein localization in plants. *Nat. Protoc* **1,** 98–103 (2006).

51. Žádníková, P. *et al.* Role of PIN-mediated auxin efflux in apical hook development of Arabidopsis thaliana. *Development* **137,** 607–17 (2010).

52. Vandenbussche, F. *et al.* The auxin influx carriers AUX1 and LAX3 are involved in auxin-ethylene interactions during apical hook development in Arabidopsis thaliana seedlings. *Development* **137,** 597–606 (2010).

53. Deplancke, B., Dupuy, D., Vidal, M. & Walhout, A. J. M. A gateway-compatible yeast one-hybrid system. *Genome Res* 2093–2101 (2004). doi:10.1101/gr.2445504.14

54. Wu, F.-H. *et al.* Tape-Arabidopsis Sandwich - a simpler Arabidopsis protoplast isolation method. *Plant Methods* **5,** 16 (2009).

55. Wehner, N. *et al.* High-throughput protoplast transactivation (PTA) system for the analysis of Arabidopsis transcription factor function. *Plant J.* **68,** 560–569 (2011).

56. Hellens, R. P. *et al.* Transient expression vectors for functional genomics, quantification of promoter activity and RNA silencing in plants. *Plant Methods* **1,** 13 (2005).

57. Heckman, K. L. & Pease, L. R. Gene splicing and mutagenesis by PCR-driven overlap extension. *Nat. Protoc.* **2,** 924–932 (2007).

58. Bowler, C. *et al.* Chromatin techniques for plant cells. *Plant J.* **39,** 776–789 (2004).

FIGURE LEGENDS

Figure 1: **Truncation of *PIN7* promoter results in cytokinin-insensitive *PIN7* transcription.** (**a-e**) Expression of *GFP* (a,b) and *PIN7-GFP* (c,d) is upregulated in response to cytokinin when driven by the full *PIN7* (a,c), but not the truncated *ΔPIN7* (b,d) promoter. Green: nuclear-localized *GFP* (a,b); membrane-localized *PIN7-GFP* (c,d). A semi-quantitative color-coded heat-map of the GFP fluorescence intensity is provided. Quantification of *PIN7-GFP* in the provasculature of primary roots (e). Roots of 7-day-old seedlings (n=15) were treated with control Murashige and Skoog (MS) medium with or without 5 μM of the cytokinin (CK) N6-benzyladenine for 8 h. Student's t-test (***p<0.001, n= 15). (**f-j**) Seedlings expressing *ΔPIN7::PIN7-GFP* in the *pin7* background exhibit enhanced root growth (f,h) and reduced cytokinin sensitivity of primary root growth (f,g,h), root meristem (RM) size (i) and lateral root initiation (j). Seedlings were grown for 28 (f,g), 14 (h), and 7 days (h,i,j) on MS medium with or without following cytokinins: 0.025 μM N6-benzyladenine (f-h); 0.025, 0.05 and 0.1 μM N6-benzyladenine (i) and 0.025 and 0.05 μM N6-benzyladenine (j). Student's t-test (*p<0.05;**p<0.01; ***p<0.001 (h,j); or *p<0.01;**p<0.001; ***p<0.0001 (i); n=10-15). *ΔPIN7::PIN7-GFP_1* and *ΔPIN7::PIN7-GFP_2* represent two independent transgenic lines

crossed into the *pin7* mutant background. Error bars represent standard error. Scale bars, 20 µm (a-d), 2 cm (f-g).

Figure 2: Cytokinin response factors (CRFs) interact with *PCREs*. (**a, b**) CRF2, CRF3 and CRF6 interaction with *PCRE7* (a) and *PCRE1* (b) results in HIS3 reporter activation in a Y1H assay in contrast to AP2-79 that does not interact. Yeast cells were grown on SD-H-U-T minimal media without histidin (H), uracil (U) and tryptophan (T), supplemented with 3- amino-1,2,4-triazole (3AT). (**c, d**) Interaction of CRF2 (c) and CRF6 (d) with *PCRE1* and *PCRE7* detected by chromatin immunoprecipitation (ChIP). Chromatin immunoprecipitated with anti-GFP antibody is enriched in the *PCRE1* and *PCRE7* region. No enrichment was detected with *PIN7* [-553-357] and *PIN1* [-512-433] elements. (**e-f**) Significantly upregulated expression of *PIN1::LUC* and *PIN7::LUC*, by co-expression with *CRF2* (e) and *CRF6* (f) in contrast to their truncated counterparts (*ΔPIN1::LUC*, *ΔPIN7::LUC*) in *Arabidopsis* mesophyll protoplasts, Student's t-test (*p<0.01, n=3). (**g**) ChIP of CRF6-GFP reveals a significantly higher enrichment for regions either containing (P1_2) or directly neighboring (P1_3) the *AGCAGAC* motif when compared to more distant regions in *PCRE1* (P1_1 and P1_4) (*** p<0.0001, n=3) (h). CRF6 increases expression of *PIN2* promoter containing three *G2G5C7* motifs in *Arabidopsis* root cell suspension protoplasts (*p<0.01, n=5) (h). Error bars represent standard error (protoplast assay) and standard deviation (ChIP).

Figure 3: Expression of *PIN* genes is altered in *CRF*-overexpressing lines. (**a,b**) *PIN7::PIN7-GFP* expression is upregulated in the provasculature of *CRF2* and *CRF6*, but downregulated in *CRF3*-overexpressing lines. (**c,d**) *ΔPIN7::PIN7-GFP* is not upregulated in the *CRF2*-overexpressing line in either absence or presence of cytokinin (5 µM N6- benzyladenine for 5 h). The membrane PIN7-GFP signal was quantified in the pericycle (b,d). Student's t-test (*p<0.05, **p<0.01; ***p<0.001, n =15-20). (**e**) *PIN7* expression in lines overexpressing CRFs monitored by qRT-PCR, no expression detected in *pin7* mutant (*p<0.05; ***p<0.0001, n = 3). Error bars represent standard error. Seven-day-old seedlings were analyzed.

Figure 4: *Crf* mutants exhibit defective embryogenesis and root development. (**a**) Auxin accumulation in the root tip of *crf3crf6* mutants. (**b-i**) Abnormal divisions of upper suspensor

cells, embryo proper, and occasionally double embryos were observed in embryos of *crf2* (c), *crf3* (f) and *crf3crf6* (d,g,h) loss-of-function mutants when compared with controls (b,e,i). (**j-n**) Lack of *crf2*, *crf3*, *crf6* as well as *crf3crf6* and *crf2crf3crf6* function affects root length (j,l), root meristem size (k,m), and lateral root primordia density (n) and their response to cytokinin. (**o-r**) Constitutive expression of *CRF2*, *CRF3* and *CRF6* affects root growth (o), root meristem size (p) and lateral root initiation density (r) and their response to cytokinin. Seedlings were grown for 7 days on control MS medium with or without 0.05 μM of the cytokinin (CK) N6-benzyladenine (l-r). Student's t-test (*p<0.05; **p<0.01; ***p<0.001; n=10-15). Arrows indicate the distance between the quiescent center (QC) and the cortex transition zone (k). Error bars represent standard error. Scale bars, (j) 2 cm, (k) 20 μm.

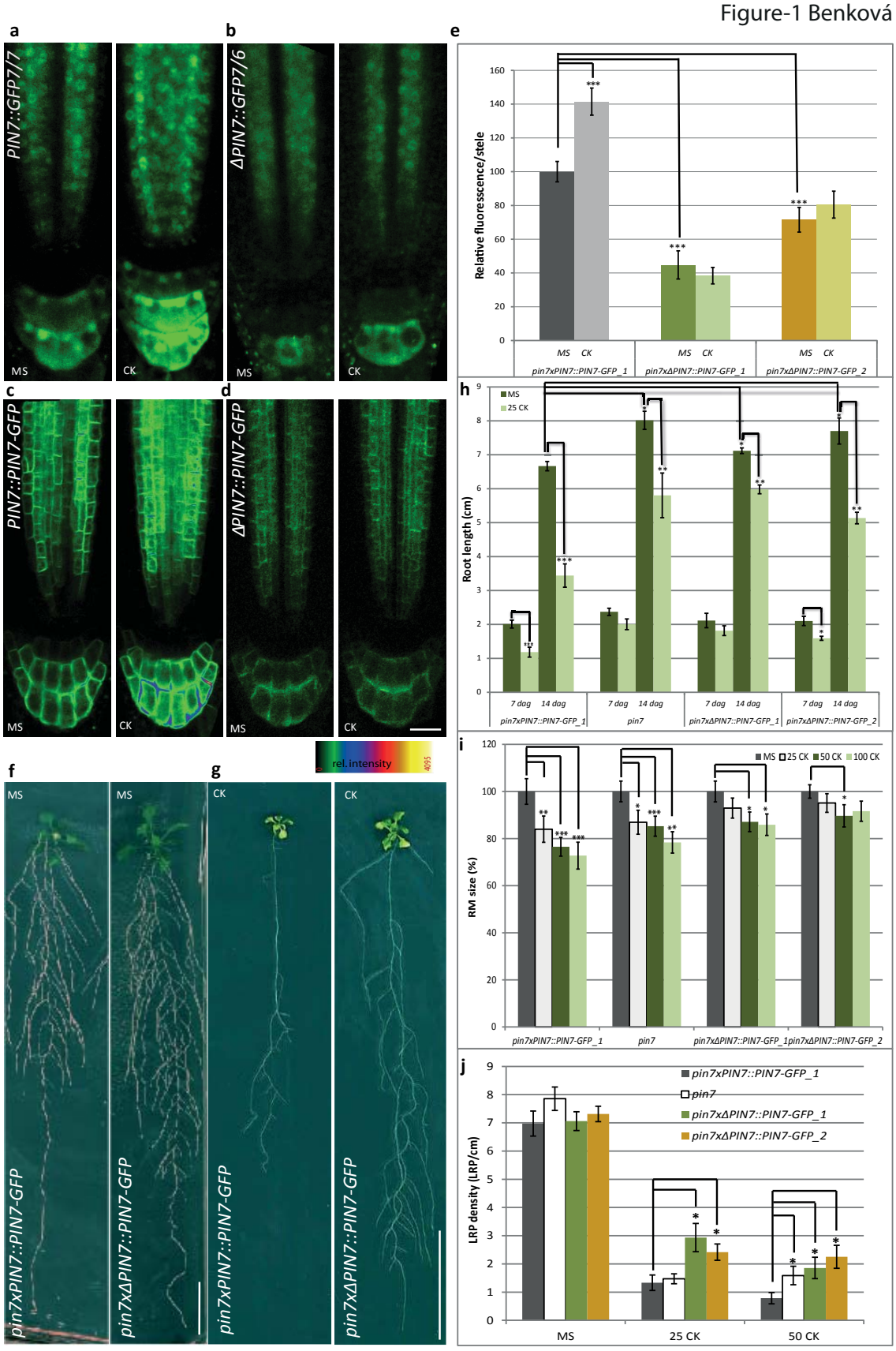
a
b
e
PIN7::GFP7/7
ΔPIN7::GFP7/6
MS
CK
MS
CK
Relative fluoresscence/stele
MS CK
pin7xPIN7::PIN7-GFP_1
MS CK
pin7xΔPIN7::PIN7-GFP_1
MS CK
pin7xΔPIN7::PIN7-GFP_2
c
d
h
PIN7::PIN7-GFP
ΔPIN7::PIN7-GFP
MS
25 CK
Root length (cm)
7 dag 14 dag
pin7xPIN7::PIN7-GFP_1
7 dag 14 dag
pin7
7 dag 14 dag
pin7xΔPIN7::PIN7-GFP_1
7 dag 14 dag
pin7xΔPIN7::PIN7-GFP_2
rel.intensity
f
g
i
MS
CK
MS 25 CK 50 CK 100 CK
RM size (%)
pin7xPIN7::PIN7-GFP_1
pin7
pin7xΔPIN7::PIN7-GFP_1
pin7xΔPIN7::PIN7-GFP_2
pin7xPIN7::PIN7-GFP
pin7xΔPIN7::PIN7-GFP
j
pin7xPIN7::PIN7-GFP_1
pin7
pin7xΔPIN7::PIN7-GFP_1
pin7xΔPIN7::PIN7-GFP_2
LRP density (LRP/cm)
MS
25 CK
50 CK

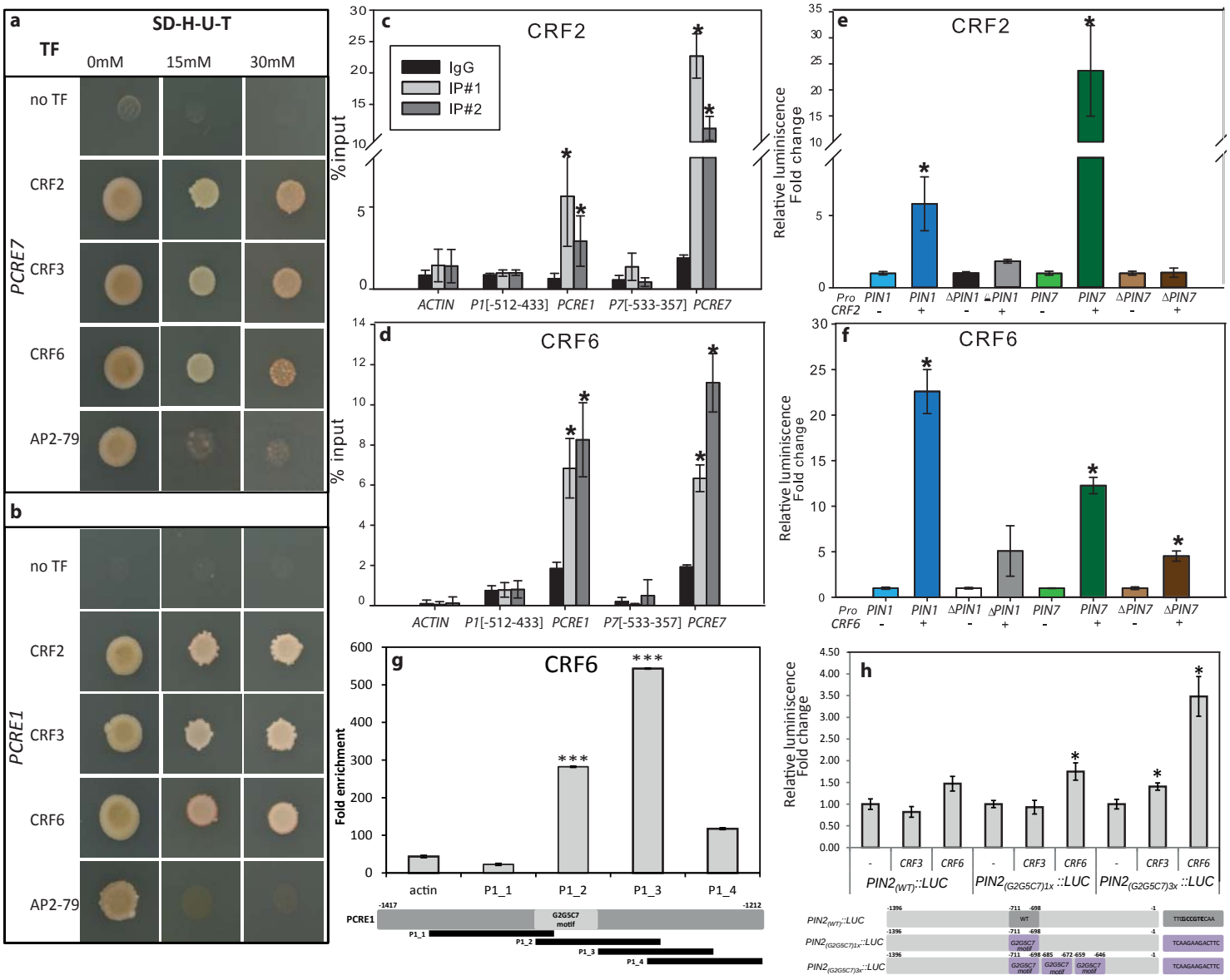
a
SD-H-U-T
TF
0mM
15mM
30mM
no TF
CRF2
CRF3
CRF6
AP2-79
PCRE7
b
no TF
CRF2
CRF3
CRF6
AP2-79
PCRE1
c
CRF2
IgG
IP#1
IP#2
% input
ACTIN
P1[-512-433]
PCRE1
P7[-533-357]
PCRE7
d
CRF6
% input
ACTIN
P1[-512-433]
PCRE1
P7[-533-357]
PCRE7
e
CRF2
Relative luminiscence
Fold change
Pro CRF2
PIN1
ΔPIN1
PIN7
ΔPIN7
f
CRF6
Relative luminiscence
Fold change
Pro CRF6
PIN1
ΔPIN1
PIN7
ΔPIN7
g
CRF6
Fold enrichment
actin
P1_1
P1_2
P1_3
P1_4
PCRE1
G2G5C7 motif
h
Relative luminiscence
Fold change
CRF3
CRF6
PIN2(WT)::LUC
PIN2(G2G5C7)1x::LUC
PIN2(G2G5C7)3x::LUC
WT
TTGCCGTCAA
TCAAGAAGACTTC

Figure-3 Benková

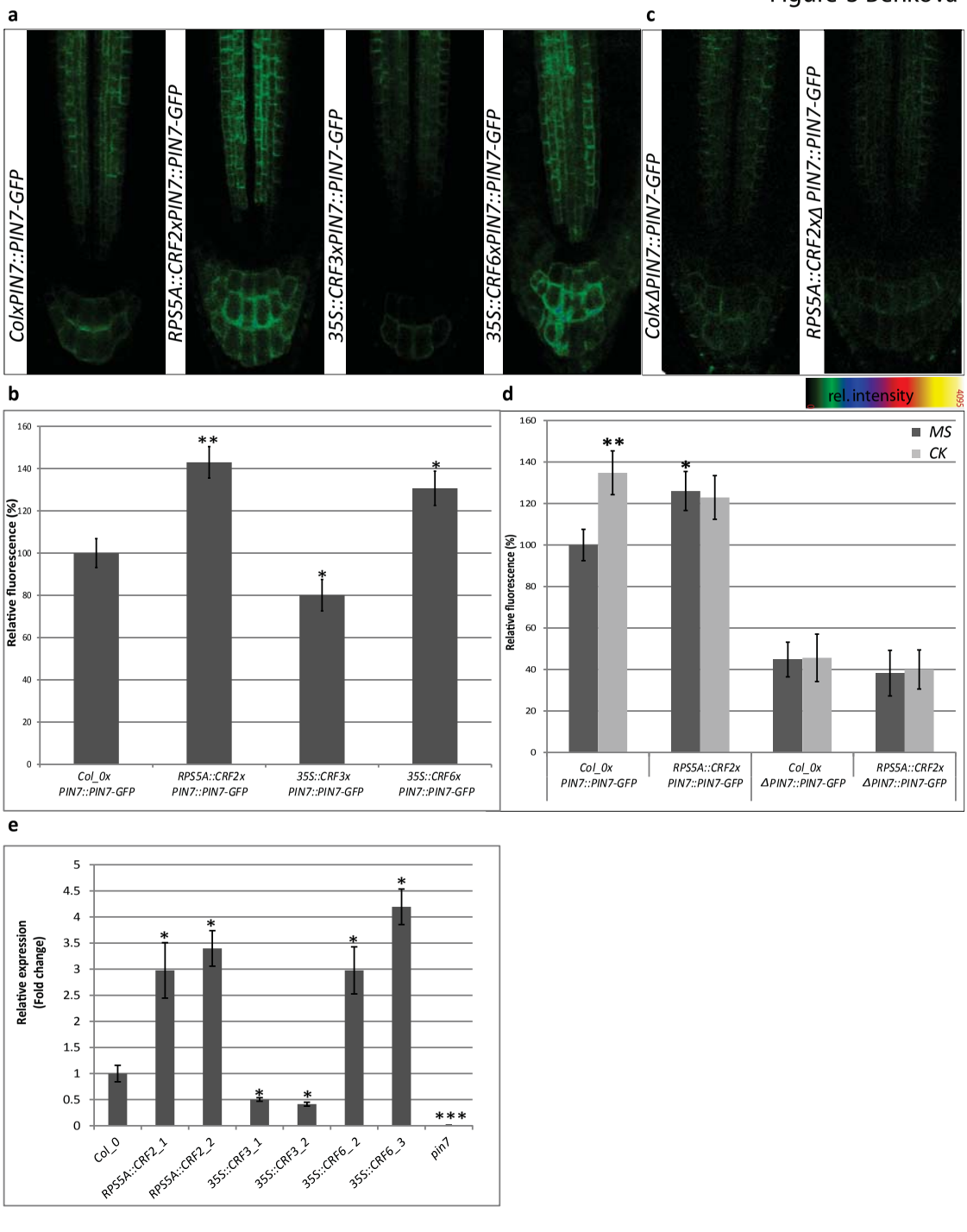

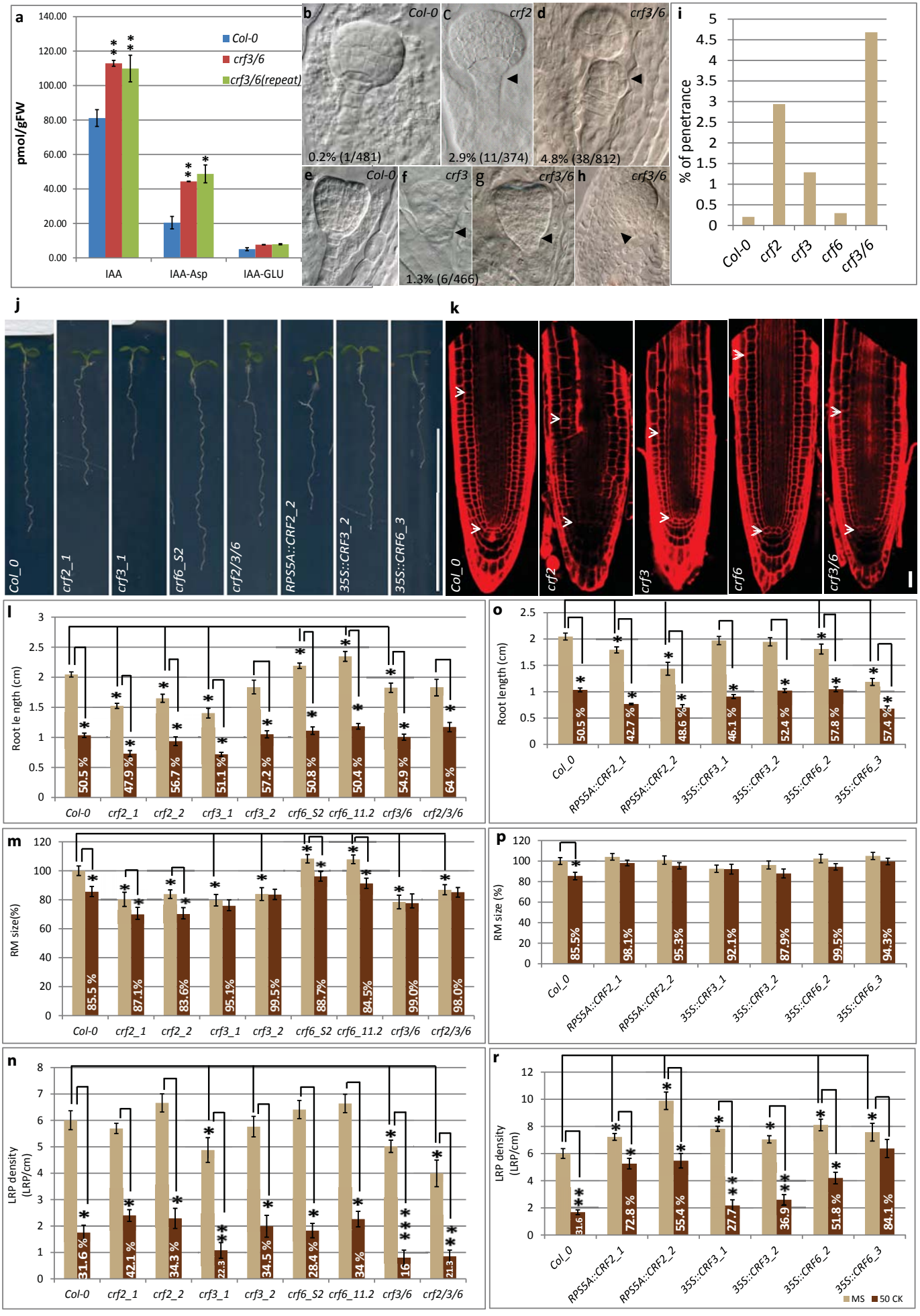
a
pmol/gFW
Col-0
crf3/6
crf3/6(repeat)
IAA
IAA-Asp
IAA-GLU
b Col-0
c crf2
d crf3/6
0.2% (1/481)
2.9% (11/374)
4.8% (38/812)
e Col-0
f crf3
g crf3/6
h crf3/6
1.3% (6/466)
i
% of penetrance
Col-0
crf2
crf3
crf6
crf3/6
j
Col_0
crf2_1
crf3_1
crf6_S2
crf2/3/6
RPS5A::CRF2_2
35S::CRF3_2
35S::CRF6_3
k
Col_0
crf2
crf3
crf6
crf3/6
l
Root le ngth (cm)
50.5 %
47.9 %
56.7 %
51.1 %
57.2 %
50.8 %
50.4 %
54.9 %
64 %
Col-0
crf2_1
crf2_2
crf3_1
crf3_2
crf6_S2
crf6_11.2
crf3/6
crf2/3/6
o
Root length (cm)
50.5 %
42.7 %
48.6 %
46.1 %
52.4 %
57.8 %
57.4 %
Col_0
RPS5A::CRF2_1
RPS5A::CRF2_2
35S::CRF3_1
35S::CRF3_2
35S::CRF6_2
35S::CRF6_3
m
RM size(%)
85.5 %
87.1%
83.6%
95.1%
99.5%
88.7%
84.5%
99.0%
98.0%
p
RM size (%)
85.5%
98.1%
95.3%
92.1%
87.9%
99.5%
94.3%
n
LRP density (LRP/cm)
31.6 %
42.1 %
34.3 %
22.3
34.5 %
28.4 %
34 %
16
21.3
r
LRP density (LRP/cm)
31.6
72.8 %
55.4 %
27.7
36.9
51.8 %
84.1 %
MS
50 CK